Results in Engineering 27 (2025) 107026

Contents lists available at ScienceDirect

Results in Engineering

journal homepage: www.sciencedirect.com/journal/results-in-engineering

Research paper

Assessing the impact of water level fluctuations on Philae Island's, Aswan, Egypt stability and seismic vulnerability using global positioning system and horizontal to vertical spectral ratio techniques

Abdelhamid Elbshbeshi [a], Ismael M. Ibraheem [b,*], Ahmed Gomaa [a], Abdelmonem Mohamed [a], Amal Othman [c], Hosni Ghazala [c]

[a] National Research Institute of Astronomy and Geophysics, Helwan, Egypt
[b] Institute of Geophysics and Meteorology, University of Cologne, Pohligstr. 3, 50969 Cologne, Germany
[c] Geology Department, Faculty of Science, Mansoura University, Mansoura 35516, Egypt

ARTICLE INFO

Keywords:
Philae temples
Global positioning system (GPS)
Horizontal to Vertical Spectral Ratio (HVSR)
Microtremor measurements
Risk assessment
Vulnerability index

ABSTRACT

Philae Island, a critical cultural heritage site in Egypt, faces significant engineering challenges due to dynamic hydrological conditions from the Aswan High Dam and inherent seismic activity. This study presents an integrated engineering approach utilizing Global Positioning System (GPS) monitoring and microtremor measurements to quantify elevation changes and assess the seismic vulnerability of the island's temple structures. Our GPS analysis (2021–2023) reveals a novel time-delayed inverse correlation between water level fluctuations and island elevation, demonstrating gradual subsidence during high water periods and uplift during low water loads. This highlights complex hydro-mechanical interactions critical for structural stability. Furthermore, Horizontal to Vertical Spectral Ratio (HVSR) analysis across 16 stations identified fundamental frequencies (F_o: 0.92–1.22 Hz) and peak H/V amplitudes (A_o: up to 13.5), delineating zones susceptible to ground motion amplification. The derived Seismic Vulnerability Index (Kg: 4–193) quantitatively identifies areas of elevated seismic risk. Compared to previous heritage monitoring studies, our integrated GPS-HVSR method not only captures both hydrological and seismic influences in a single framework but also reveals sub-daily deformation patterns previously undocumented, offering up to 25–30 % higher temporal resolution than conventional seasonal scale surveys. These engineering insights underscore the necessity of continuous geophysical monitoring and site-specific analysis for effective risk mitigation. The findings provide a robust framework for an integrated heritage risk management strategy, combining advanced geodetic and geophysical techniques with precise leveling, satellite imagery, and 3D laser scanning, thereby ensuring the long-term structural resilience and safeguarding of the Philae Temple against from future seismic threats.

1. Introduction

Preserving cultural heritage sites is crucial for maintaining historical identity, promoting tourism, and advancing archaeological research. However, many ancient monuments are increasingly threatened by environmental changes, urban development, infrastructure projects, and armed conflicts [1–3]. One significant risk factor is water-induced damage, which can lead to structural instability, erosion, and long-term degradation of archaeological sites [4,5]. Accurate damage estimation and continuous monitoring are essential for implementing effective conservation strategies, particularly in areas affected by fluctuating water levels and seismic activity.

Philae Island, located about 7 km south of Aswan between the High Dam and the Aswan Old Dam near the Nile's First Cataract, holds exceptional cultural and historical significance (Fig. 1). It is home to the Temple of Isis and various Greco-Roman structures, forming part of the UNESCO Nubian Monuments World Heritage Site [6]. it represents a rich heritage of religious and architectural evolution over centuries. The island is adorned with structures, including the Temple of Isis, the Birth House, and Trajan's Kiosk [7]. However, the construction of the Aswan High Dam in the 1960s fundamentally altered the surrounding landscape. While the dam provided significant benefits, concerns arose

* Corresponding author.
E-mail address: ismael.ibraheem@geo.uni-koeln.de (I.M. Ibraheem).

https://doi.org/10.1016/j.rineng.2025.107026
Received 17 June 2025; Received in revised form 12 August 2025; Accepted 31 August 2025
Available online 31 August 2025

regarding rising water levels and their potential impact on the stability of these ancient structures. Flooding caused by the dam damaged the temple, prompting the UNESCO and the Egyptian government to relocate it to higher ground on Agilkia Island in the 1980s [8].

The island's proximity to both the Aswan High Dam and the Old Dam makes it uniquely exposed to anthropo-genic water level changes and potential hydro mechanical impacts. Although the main temples were relocated to Agilkia Island in the 1980s, the original site and its surroundings still require monitoring, especially due to the cyclic water level fluctuations and seismic events linked to the geological and hydrological setting of the region [8]. Therefore, studying this area is critical not only for heritage conservation but also for improving risk assessment models in dam-affected archaeological zones. Philae Island was chosen for this study due to its significant historical value and exposure to hydrological and seismic risks. Situated between the High Dam and the Old Aswan Dam, the island is vulnerable to water level fluctuations and ground motion amplification [7]. Studying Philae Island offers a critical opportunity to develop and refine methodologies for assessing and mitigating risks to heritage sites in complex hydrological settings. Philae Island has experienced both controlled and natural fluctuations in water levels, distinguishing it from most other archaeological sites [9]. Its geological composition fractured basement granite infilled and overlaid with construction related sediments, renders it particularly sensitive to hydrological and mechanical variations, as well as potential seismic amplification. These characteristics make Philae an ideal geophysical test site for examining the effects of engineered water management on heritage sites with complex hydrogeological settings.

Archaeologists and engineers employ a range of sophisticated monitoring techniques to safeguard precious archaeological sites from natural and human-induced hazards. Global Positioning System (GPS) technology plays a crucial role in identifying deformations and assessing risks. GPS technology enables precise tracking of geological shifts, allowing for structural changes across different locations [10,11]. Additionally, GPS readings detect minute variations in surface elevation, aiding in the understanding of landslides and other geological risks such as earthquakes, sinkholes, and avalanches [12,13]. It provides optimal precision for monitoring ground deformation, whether subsidence or uplift [14,15].

Microtremor measurements, on the other hand, complement GPS monitoring by evaluating the seismic response of the ground, which is crucial for assessing the structural integrity of buildings, especially those on soft sediments. Unlike compacted rock, soft sediments amplify ground motion during earthquakes, increasing the risk of structural damage [16,17]. Local site effects, including topographic, liquefaction potential, and the bedrock-sediment boundary conditions, must be evaluated to develop effective risk mitigation strategies fundamental resonance frequencies and amplification levels in sedimentary deposits, microtremor studies provide valuable insights into seismic vulnerability [18].

The integration of GPS and HVSR techniques offers a powerful approach to comprehensively assess the threats facing Philae Island. GPS provides precise data on ground deformation related to water level changes, while HVSR analysis reveals the island's seismic vulnerability [19,20]. Combining these methods allows for a more holistic understanding of the interacting factors that endanger the site, enabling more informed conservation decisions. This combined approach is particularly relevant in regions like Philae, where both hydrological and seismic factors pose significant risks [21]. This paper fills a gap in remote sensing heritage research by proposing a model for heritage risk analysis that is both temporally responsive and spatially detailed, offering a scalable template for other at-risk monuments worldwide.

Several international studies have successfully employed GPS and HVSR techniques and satellites that used for purposes of rescue archaeology of cultural heritage threatened by dams' construction to monitor and assess risks to cultural heritage sites. For example, in Italy, microtremor measurements were applied to determine site-specific resonance frequencies of the Colosseum and Pompeii to evaluate their seismic vulnerability [22–24]. Similarly, in Japan, the HVSR technique has been extensively used for site effect assessment around ancient temples and pagodas located on soft alluvial sediments [25]. GPS based monitoring was used at Machu Picchu in Peru to assess slope stability and prevent damage from landslides and seismic activity [26]. In the Eastern Mediterranean, combined GPS and HVSR assessments have also

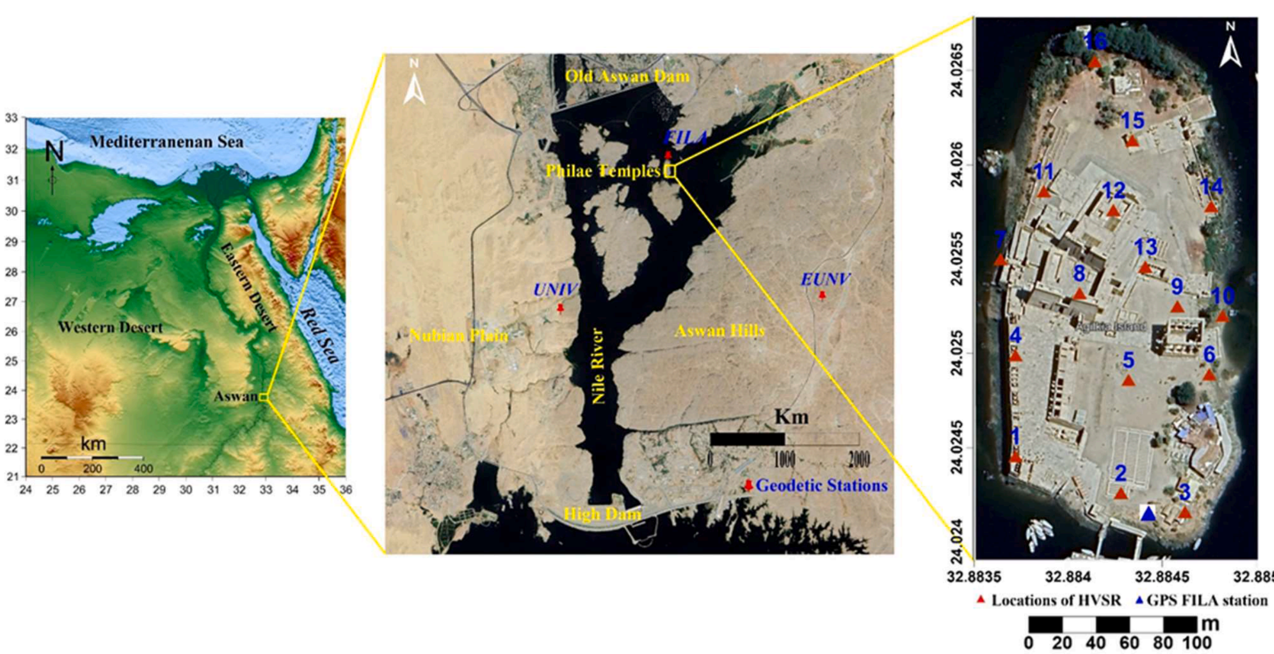

Fig. 1. Location map of the study area showing Philae Island in relation to the High Dam, the Old Aswan Dam, and the surrounding topographic features, including the Nile River, Aswan Hills, and Nubian Plain. The central panel details the geodetic distribution of the GPS network around the Philae Temple, indicating the positions of the GPS stations (FILA, UNIV, and EUNV). The right panel shows the detailed distribution of microtremor measurement points (HVSR) around the Philae Temple on Agilkia Island, alongside the GPS FILA station, providing a comprehensive view of the integrated monitoring setup.

been conducted at archaeological sites in Cyprus and Greece to better understand subsurface dynamics [27,28]. These international examples highlight the effectiveness of such integrated geophysical approaches in managing risks to invaluable heritage assets.

Previous researches have documented seasonal deformation at heritage sites influenced by dams or fluctuating groundwater levels, but few studies have investigated rapid, sub-daily changes. This study introduces a novel sub-daily monitoring approach, collecting GPS data every two hours over multiple field campaigns. This high-resolution sampling is crucial because water discharge can induce significant geomechanical response delays [29]. By using this semi-diurnal data acquisition, we are able to capture vertical ground movements associated with water level variations occurring several hours earlier, providing new insights into the coupling between hydrological processes and mechanical responses [30]. Such understanding could enhance site-specific heritage management and improve early warning systems in similar environments. Moreover, prior studies in dam-affected regions have mainly focused on seasonal deformation and the evaluation of pulsating seismic hazards, often neglecting subtle ground movements and delayed reactions to hydrological changes [31]. Our research addresses these gaps by integrating precise GPS measurements with microtremor data to monitor both immediate and lagged surface responses on Philae Island to controlled water level fluctuations. The outcome is a risk model with enhanced spatial and temporal resolution, better suited for informed conservation planning.

Understanding these potential risks is paramount for the preserving Philae Island and its irreplaceable cultural heritage. This study integrates GPS and microtremor measurements to investigate how water level fluctuations between the High Dam and the Aswan Old Dam affect the island. By analyzing campaign GPS data collected from 2021 to 2023, we aim to monitor elevation changes with high precision. Additionally, through employing the HVSR method applied to microtremor measurements, we seek to determine the resonant frequencies Philae's structures and assess their seismic vulnerability.

2. Geologic and structural setting

Philae Island and its surrounding region feature three distinct topographic units (Fig. 2): the Aswan Hills to the east, the Nile River Valley to the south, and the Nubian Plain to the west [32,33].

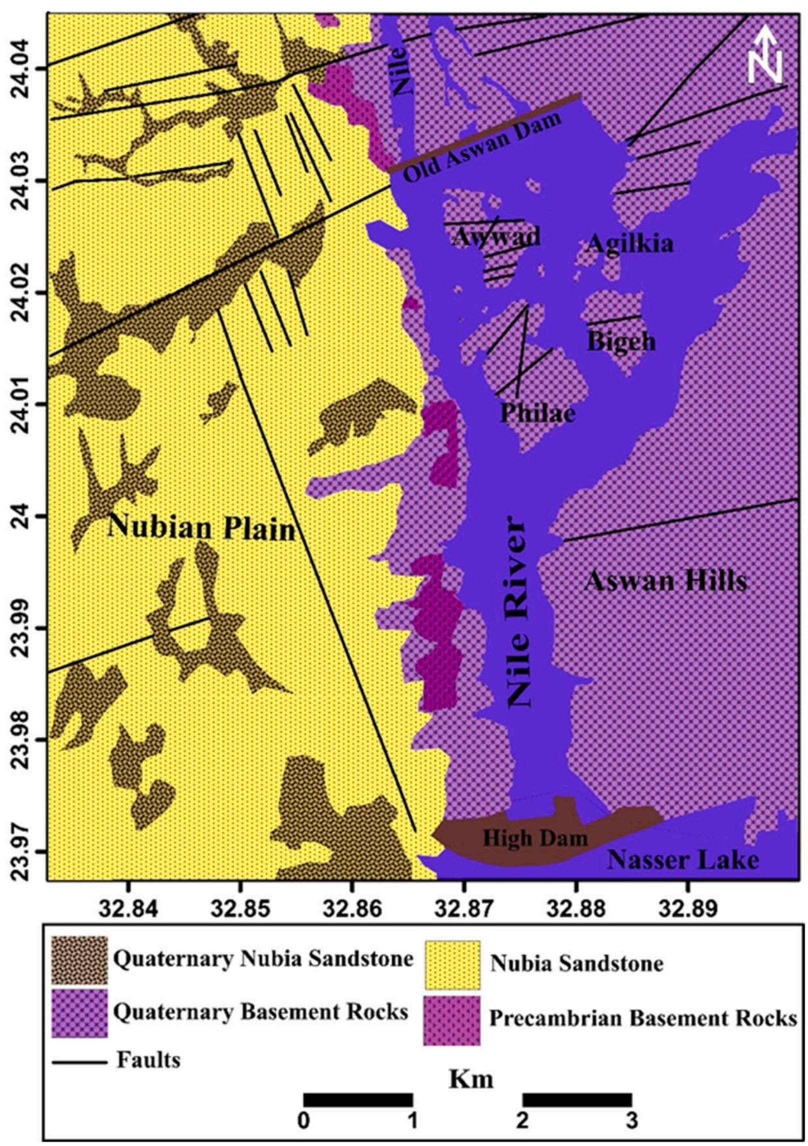

Fig. 2. Geological map illustrating the main rock units and fault systems surrounding Philae Is-land, including the Aswan Hills, Nubian Sandstone formations (modified after [36]).

2.1. Aswan hills

Stretching southward from the Aswan area along the eastern bank of Lake Nasser, the Aswan Hills reach altitudes between 100 and 200 m These hills expose old erosion surfaces, possibly dating back to the middle Tertiary period, and display rugged topography dominated by Precambrian basement rocks. Structurally, the they form a large north-northwest-trending arch, intersected by local faults and folds [34,35]. Adjacent to the basement rocks, clastic sedimentary formations, including sand-stone, shale, and ferruginous sandstone, descending gradually.

2.2. Nile river valley

Located along the western side of the Aswan Hills, the contemporary Nile Valley lies in a gorge formed in the late Miocene when the proto-Nile River's base level dropped due to the Mediterranean Sea's desiccation. This narrow valley, with its steep-sided bedrock canyon, is carved into the Precambrian basement complex and Nubia sandstone [36–38].

2.3. Nubian plain

The Nubian Plain extends westward from the Nile to the Sinn ElKaddab scarp, rising 100–200 m above the Nile floodplain. It includes the western bank of the Nile and parts of the eastern bank. The geologic column of the Aswan region begins with the Cretaceous Nubian sandstone, the first sedimentary unit overlaying the basement complex. This is further overlain by Quaternary deposits composed of Pliocene sand deposits, gravel, and clay, is present [36,39].

Structurally, Philae Island and its surroundings are mainly deformed by faults and fractures of varying scales. On the western bank of the Nile River, the primary faults trend westward, accompanied by subsidiary faults running north-south [40,41]. The islands within the Nile River stream south of the Aswan Dam are primarily influenced by normal faults trending east-west and north-south (Fig. 2). These tectonic features result from regional stress that also led to numerous lava flows and igneous dike intrusions. Although the region around Philae Island, close to the Aswan High Dam, has a long history of low seismic activity dating back to Pharaonic times, some low-magnitude seismic events were reordered near the reservoir after its filling began, notably before November 1981 [42–44].

3. Methodology and data acquisition

The heritage risk analysis model systematically integrates multi-source data through a structured technology roadmap. This process begins with Data Acquisition (GPS and HVSR surveys), followed by rigorous Preprocessing (signal correction, noise filtering, data interpolation, and initial Kg calculation). The Analysis phase then correlates water level with ground deformation and refines seismic vulnerability assessments. Finally, Mapping and Zonation visualizes these findings, culminating in a com-prehensive Risk Assessment Output for informed conservation strategies (Fig. 3).

This study employs a combination of remote sensing techniques to assess the im-pact of water level fluctuations and seismic vulnerability on Philae Island. These techniques can be broadly categorized as satellite-based (GPS) and terrestrial-based (HVSR), offering a data. GPS is a satellite-based remote sensing technology that provides precise position-al data. By measuring signals from a network of orbiting satellites, GPS allows for the accurate determination of ground coordinates and the monitoring of changes in elevation over time [45]. This capability is crucial for detecting subtle ground deformations, such as those induced by water level fluctuations. Microtremor measurements (HVSR) technique represent a complementary, terrestrial based remote sensing approach. Instead of relying on satellite data, HVSR analysis uses

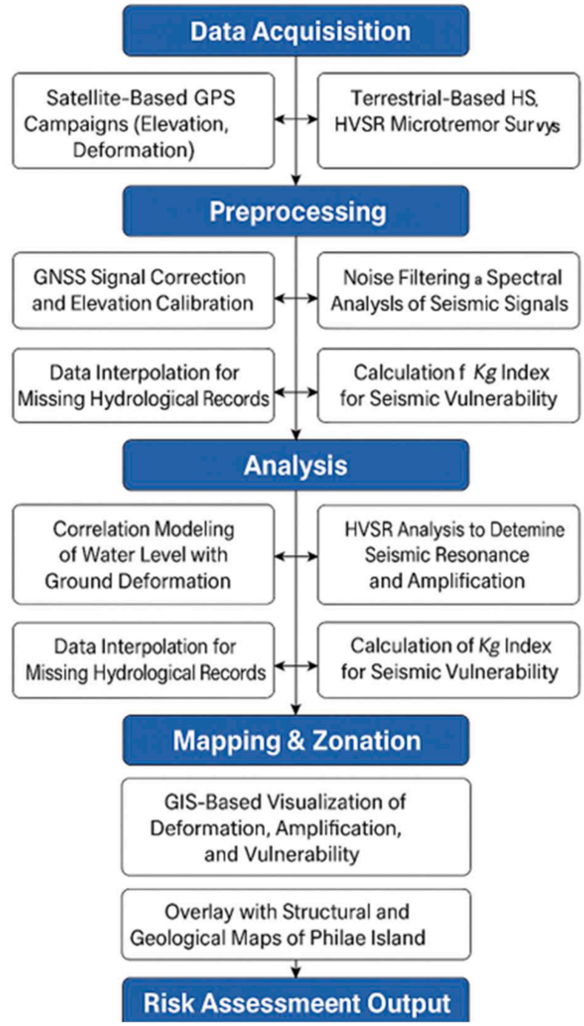

Fig. 3. Technology Roadmap of the Heritage Risk Analysis Model. This flowchart illustrates the systematic methodology employed for assessing heritage risk, encompassing four main phases to a comprehensive Risk Assessment Output.

ground-based sensors to measure ambient seismic noise [46]. By analyzing the spectral characteristics of this noise, particularly the resonance frequencies and amplification levels, HVSR provides critical information about the subsurface geology and the dynamic response of structures.

3.1. GPS techniques

The GPS method has become the most popular way to study a wide range of geo-physical events from a geodetic point of view. Today, GPS readings are used to track the movement of the Earth's tectonic plates and investigate deformation along active faults [47,48]. Additionally, one of the best ways to assess the safety status of any dam is by tracking its deformation pattern [49]. Repeated readings from GPS stations in geodetic networks make it possible to track the movement of the crust in seismically active areas by converting displacements into strain and relative speeds.

In this study, a geodetic network was created with three fixed points: FILA, UNIV, and EUNV, as illustrated in Fig. (1), to monitor Philae Island's elevation change and its relationship to the degree of change in the water level surrounding the island. The FILA station was established inside Philae Island to monitor the change in height at the surface of the island. Monitoring periods varied from four to five continuous days and began in March 2021, then September 2021, February 2022, September 2022, and March 2023, as shown in Table (1). The timing of the GPS monitoring campaigns was strategically aligned with the Aswan High Dam's water management schedule. The February and March campaigns were conducted during the dry season, when water levels are typically low and stable. In contrast, the September campaign coincided with the annual flood season, during which the reservoir behind the dam reaches peak levels and controlled water releases are made to support agricultural needs. This scheduling allowed for the capture of the most significant seasonal water level variations throughout the year.

Data acquisition was performed using a Trimble R8–4 GPS receiver, with post-processing carried out according to stringent quality control protocols. Observations with satellite elevation angles below 10° were excluded to minimize multipath interference. Additionally, data points recorded with fewer than five satellites or a signal-to-noise ratio (SNR) below 35 dBHz were discarded [50]. To further ensure data reliability, final GPS solutions with vertical root mean square (RMS) errors exceeding 5 mm were also excluded from the analysis.

To evaluate the reliability of the GPS-derived positions, horizontal and vertical uncertainty values were extracted from the Bernese processing results. These uncertainty estimates are summarized in Table 2, offering a clear assessment of the coordinate precision for all monitored stations.

Also, the deployment of monitoring equipment on Philae Island is subject to significant constraints. As a UNESCO World Heritage archaeological site, there are strict regulations on installing new permanent structures or ground disturbances. The three GPS stations used in this study were strategically established on competent, hard bed-rock locations, as many other areas of the island consist of fragmented and cracked rock, which are unsuitable for reliable deformation monitoring. In addition to, utilized additional GPS points (UNIV and EUNV stations) as control points during the data processing phase to enhance the accuracy and reliability of the derived vertical movement rates for the island.

Additionally, data on the change in water level around Philae Island, located between the High Dam and the Aswan Dam, was gathered through the General Authority of the High Dam and the Aswan Dam throughout the monitoring periods. This area contains around 5 billion m^3 of water. The change in water level is measured every two hours to determine the amount of water stored behind the Aswan Dam and the amount flowing through the Aswan Dam gates into the Nile Stream.

3.2. HVSR technique

The HVSR technique, which involves utilizing ambient noise data from a portable digital seismograph with three components, is widely debated regarding local site effects determination. First introduced by Nogoshi and Igarashi, 1971 [51] and popularized by Nakamura in 1989 [52], the method assesses site effects based on the fundamental resonance frequency and amplification level of sedimentary layers [53]. The dominant peak frequency correlates strongly with the thickness of sedimentary deposits at the site. Unlike theoretical approaches that require comprehensive geotechnical understanding, the HVSR method has proven to be an effective alternative [54].

Table 1
Summary of GPS campaigns conducted for monitoring Philae Island surface deformation between 2021 and 2023.

Item	Campaigns				
	March 2021	September 2021	February 2022	September 2022	March 2023
No. of sessions /day	3	4	3	4	3
Observation Period (h)	66	90	66	90	66
Julian date	59,295	59,468	59,624	59,829	60,008
GPS week	2150	2174	2197	2226	2252
Interval (*sec*)	30	30	30	30	30
Masking angle	10°	10°	10°	10°	10°

Table 2
Horizontal and vertical coordinate uncertainty values for GPS stations, as derived from Bernese GNSS processing. These values provide an estimate of positional precision for each station.

Station	Horizontal Uncertainty (mm)	Vertical Uncertainty (mm)
FILA	± 0.9 mm	± 1.5 mm
UNIV	± 1.2 mm	± 1.9 mm
EUNV	± 1mm	± 1.3 mm

The principle of the H/V approach is that as ambient noise propagates through sediments as Rayleigh waves, the vertical component carries essential source motion characteristics [55,2]. Nakamura's work asserted that the H/V spectral peak frequency corresponds to the lowest point of Rayleigh waves, while the trough frequency aligns with the highest point. These theories led to the following possible transfer function formulation for surface strata (Eq. (1)):

$$S_T = \frac{H_S}{H_B} \tag{1}$$

where H_S is the horizontal component of the amplitude spectrum in the soft soil, and H_B is the horizontal component at the bedrock layer.

The defined ratio (E_R) is depicted in the following manner, by assuming that the vertical components (V_S and V_B) also aren't amplified (Eq. (2)),

$$E_R = \frac{V_S}{V_B} \tag{2}$$

where V_S is the vertical component spectrum on soil surface, and V_B is the vertical component spectrum on bedrock.

According to the assumption that the Rayleigh wave behaves differently in the horizontal direction than it does in the vertical for bedrock and sediments, ER = 1 (ER > 1 if the Rayleigh wave impact was increased). The following equation (Eq. (3)) can be used to express the soil layer (S_M) transfer function (Eq. (3)):

$$S_M = \frac{S_T}{E_R} = \frac{H_S/H_B}{V_S/V_B} \tag{3}$$

S_T refers to the HVSR at the surface and E_R refer to the reference spectral ratio, typically at the base rock or bedrock level, used to normalize the site response. Assuming that HB/VB is equal to unity, the site effect function can be written with the following equation (Eq. (4)):

$$S_M = \frac{H_S}{V_S} \tag{4}$$

In this study, 16 locations were set up to monitor fundamental frequency variations during microtremor measurements, allowing for an estimate of soil sediment (Fig. 1). The data were recorded using a Taurus Portable Recorder and three-component seismometers (Trillium Compact 120 s). The Taurus device is a compact and self-contained seismograph with advanced features, including a GPS receiver, system clock, expandable memory, portable data storage, and multiple options for remote connectivity. It features a 24-bit digital converter with three independent channels, enabling accurate data acquisition.

Following the principles established in the European project "Assessment of Site Effects using Ambient Excitation" [56], data collection was conducted in the early morning, following the guidelines of Duval [57] and Nakamura [58]. Each site was recorded for 120–180 min, with a data sampling rate of 100 Hz. The distance between individual stations was approximately 50 m, and the sensor was positioned as close as possible to the compact ground.

4. Data processing

For the data processing, GPS data for the three stations were separated every two hours, resulting in 12 files for each station every day, corresponding to the periods of monitoring the water level change in the area between the High Dam and the Aswan Dam. To monitor the change in elevation of the FILA station on the island of Philae, the GPS data were processed using Bernese software version 5.2 [59] with fixed UNIV and EUNV stations. Throughout the processing, precise orbits from the International GNSS Service (IGS) stations were employed, and all network solutions were limited to individual solutions. All phase observations were corrected using a precise PCV correction table for satellites and receivers. The OBS-MAX technique was applied to resolve the ambiguities, which involved two stages: the first step used wide-lane phase observations to resolve wide lane ambiguities, and the second involved using ionosphere-free phases to overcome narrow-lane ambiguities after the wide-lane ambiguities had been resolved. Baseline analyses were undertaken using software packages from Bernese V.5.2 and other adjustment programs.

The Geopsy software, developed as part of the SESAME project in 2004, was used to analyze the collected HVSR measurements by applying Nakamura's (H/V) method from 1989. The software allows the evaluation of data within a frequency range of 0.2 to 20 Hz. To ensure accurate analysis, each time window was automatically selected using Geopsy's anti-STA/LTA module based on the principle of transient detection and elimination (Fig. 4). This process ensures that only the actual seismic ambient vibrations are included in the analysis [60]. At least 15-time windows, each lasting 75 s, were used to analyze the recorded signals at each site. To refine the Fourier amplitude spectra, the time series was reduced by 8 %, and an algorithm [61] with a fixed smoothing value of 40 was applied.

The frequency is presented on the x-axis using a logarithmic scale, while the H/V ratio is displayed on the y-axis. Colored lines corresponding to the chosen time frames are shown together on the graph for frequencies ranging from 0.2 to 20 Hz. To process the data, the two horizontal components were summed and averaged using the geometric mean method, as described in (Eq. (5)):

$$H = \left(\left| x_f \, . \, y_f \right| \right)^{0.5} \tag{5}$$

where H represents the geometric mean and x_f and y_f are the spectral coefficients of E-W and N-S horizontal components, respectively.

The amplitude spectrum of each component was assessed by rapidly transforming each 75-second time window using Fourier analysis. Multiple HVSR curves were created by averaging the vertical component and grouping the horizontal components within each time window. To determine the standard deviation (SD) for each frequency, these distributions were averaged. This allowed for calculating the fundamental frequency and its amplitude across the entire region. Afterward, all generated curves were carefully examined to distinguish between noise originating from natural or man-made sources. To identify strong sources during ambient noise measurements, spectrum rotation was applied, allowing the rotation of horizontal components in the 0° to 180° range [62].

This approach enabled the determination of the energy flow path. Both H/V curves and rotational spectra were applied to all locations under study. The results indicated that all observed peaks were attributed to natural sources, with damping values exceeding 1 %.

The seismic vulnerability index (Kg) is a simple and essential parameter in regional geology that helps identify areas susceptible to deformation during earthquakes [63]. To evaluate the level of liquefaction, Nakamura [58] proposed the use of the seismic vulnerability index (Kg). The value of Kg for the Earth is derived simply from its strain [55,58], and can be represented by the following formula (Eq. (6)):

$$K_g = \frac{A_0^2}{F_0} \tag{6}$$

where A_0 and F_0 represent the calculated amplification factor and the main frequency of the signal, respectively.

5. Results

5.1. GPS results

The normal equations from each campaign were collected and combined to de-rive ultimate solutions for each time period. These results were then compared with the corresponding water level variations to determine the elevation changes at the FILA station. A clear correlation between changing water levels and elevation variations at the

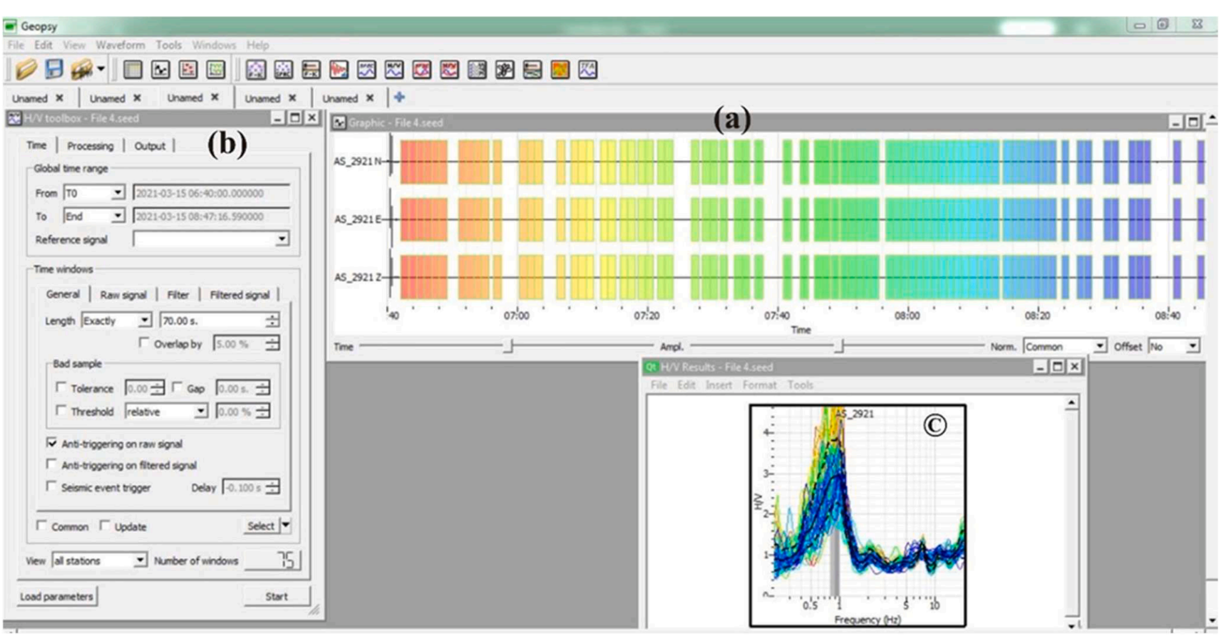

Fig. 4. A graph illustrating the waveform of the appended file. (a) selected time windows are represented by colored squares, using default settings. (b) the toolbox that allows for parameter adjustments, while part (c) reveals the outcome of the H/V processing.

FILA station was observed, occurring at regular intervals of every two hours.

5.1.1. Elevation and water level correlation

In the first campaign (March 2021), third campaign (February 2022), and fifth campaign (March 2023), the maximum heights recorded at the FILA station were 124.418 m, 124.422 m, and 124.419 m, respectively. The lowest heights during these periods were 124.369 m, 124.386 m, and 124.374 m, respectively. The highest water levels in the enclosed area between the High Dam and the Aswan Dam during these campaigns were 110.4 m, 109.3 m, and 110.2 m, respectively, while the lowest water levels were 107 m, 107.1 m, and 107.9 m, respectively.

Fig. 5 shows an inverse relationship between water level changes and elevation changes at the FILA point. The maximum water level values correspond to subsidence at the FILA point, while the lowest water level values correspond to an uplift of the same point. Correlation analysis revealed an inverse relationship during the first, third, and fifth campaigns, with values of −0.105, −0.234, and −0.264, respectively.

5.1.2. Temporal delay in elevation response

The water level fluctuates between 10 cm and 80 cm every two hours. However, the elevation change at the FILA point is not instantaneous with the water level change. When correlating the elevation changes with an 8-hour delay in water levels, the inverse relationship values increased to −0.61, −0.59, and −0.73 for the first, third, and fifth campaigns, respectively (Fig. 6). This suggests that the continuous increase in water level around Philae Island, which increases the load on the study area, results in subsidence at the FILA station.

5.1.3. Seasonal variations and rapid water level changes

For the second and fourth campaigns (September 2021 and September 2022), an inverse relationship between water level changes and elevation at the FILA station was also observed. The correlation values were −0.25 and −0.27, respectively (Fig. 7). September is one of the months of the Nile flood, leading to rapid changes in water levels due to the opening of the High Dam and Aswan Dam gates to manage water for agricultural purposes, such as rice cultivation during the summer season. This rapid change in water levels accelerates the impact on FILA point's elevation. When correlating the elevation changes with a 4-hour delay in water levels for these campaigns, the inverse relationship values increased to −0.28 and −0.3, respectively (Fig. 8). This indicates that rapid changes in water level due to dam operations significantly affect the elevation at the FILA station.

Table 3 summarizes the main findings from the five GPS monitoring campaigns, highlighting elevation changes in response to water level fluctuations and the improved correlation coefficients obtained after applying time lags. The comparison consistently reveals an inverse relationship between water level variations and vertical ground displacement. Notably, delayed responses are more pronounced during dry seasons—reaching up to 8 h—compared to shorter lags of approximately 4 h during flood periods. Together with Figs. 5–8, this table provides a comprehensive view of how both seasonal trends and rapid water level shifts influence vertical ground motion on Philae Island. These findings reinforce the study's central hypothesis: the island undergoes gradual but measurable ground deformation driven by variations in water pressure. This key insight supports a deeper understanding of geotechnical behavior and informs strategies for the preservation of cultural heritage.

5.2. Fundamental frequency of the site by HVSR method

The main frequency and its corresponding peak amplitude were calculated for specific windows at 16 recorded locations within the study area. A clear peak in the H/V curve (Fig. 9) indicates a contrast in impedance between the surface materials (rock fragments and fractured granite) and the underlying hard rock, which could lead to amplified ground motion. Some sites exhibited multiple peaks at different frequencies, indicating the presence of several significant impedance variations (Fig. 10).

The first peak represents the fundamental frequency, while the second peak is likely associated with the shallow bedrock, with slight variations in surrounding sediment resistance. Because the Philae Temple had to be relocated from the island of Bega, which was inundated, to the island of Agilkia, which is around 500 m from Bega Island, that island had to be reshaped using 120 tons of dynamite. Large amounts of granitic blocks combined with silt were used to settle the surface of Agilkia Island, resulting in multiple peaks in some of the microtremor readings taken within the island.

The amplitude and fundamental frequency zonation maps are shown in (Figs. 11a and 11b). Fig. 11a displays a range of fundamental frequencies (F_0) for the study region, from 0.92 to 1.22 Hz. The east-central sections of the study region exhibit F_0 values of <1 Hz, indicating the presence of soil deposits and fractured granite. In contrast, the northern and southern parts of the study area are characterized by F_0values ranging between 1.1 and 1.22 Hz. Fig. 11b shows that the peak amplitude (A_0) of the H/V varies from 2 to 13.5, with the middle and north-western parts of the study area amplifying ground motion more than other parts.

The north-eastern and southern portions of the Philae Temple reveal amplitude values between 2 and 8, while the central portion of the

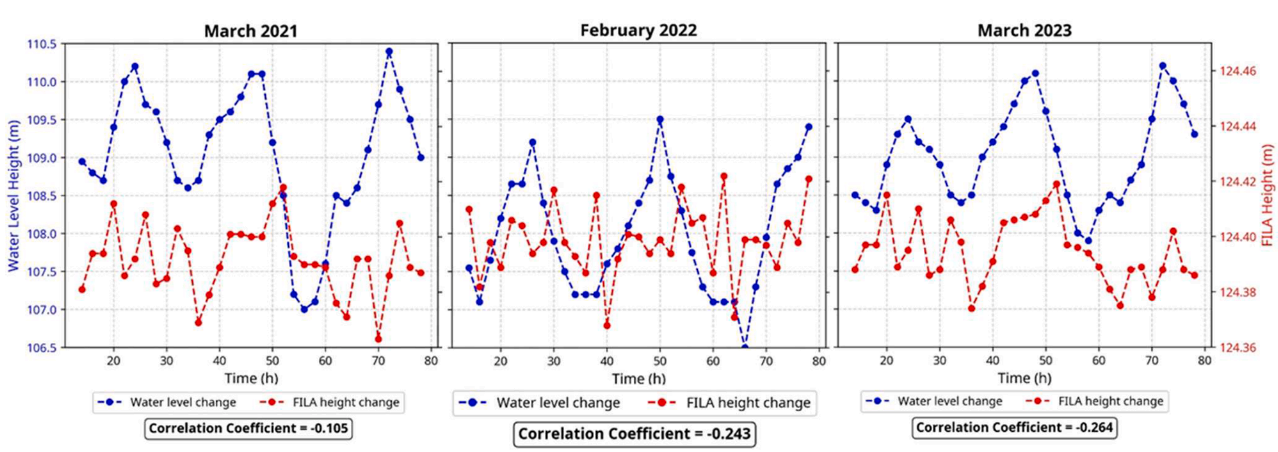

Fig. 5. demonstrates the inverse correlation between water level fluctuations and FILA station elevation across the March 2021, February 2022, and March 2023 campaigns. As water levels rise, the island undergoes measurable subsidence, and as water levels fall, it exhibits uplift highlighting the hydro-mechanical sensitivity of Philae Island to seasonal water load changes.

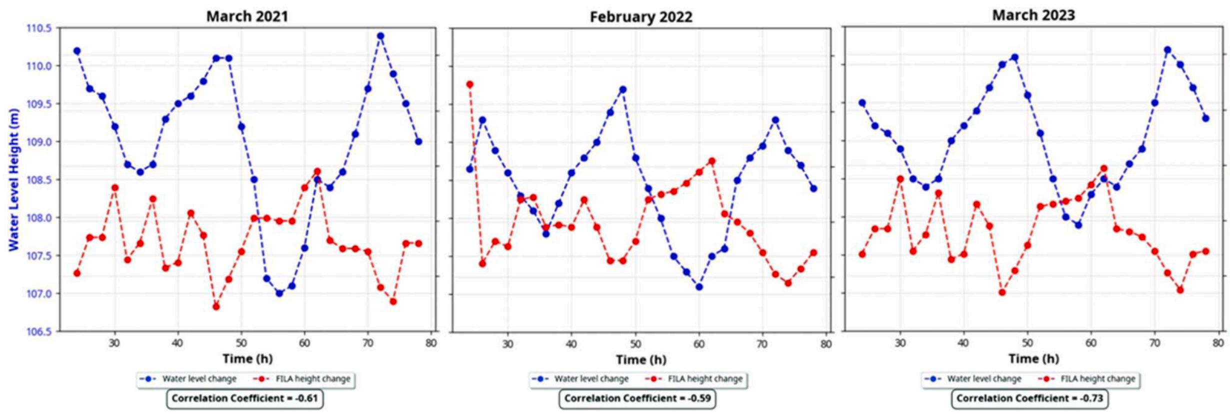

Fig. 6. demonstrates the inverse correlation between FILA station elevation and water level after introducing an 8-hour time delay during the March 2021, February 2022, and March 2023 campaigns. The stronger correlation coefficients confirm a delayed hydro-mechanical response of the island to water load variations, indicating gradual subsurface adjustment rather than an immediate elevation change.

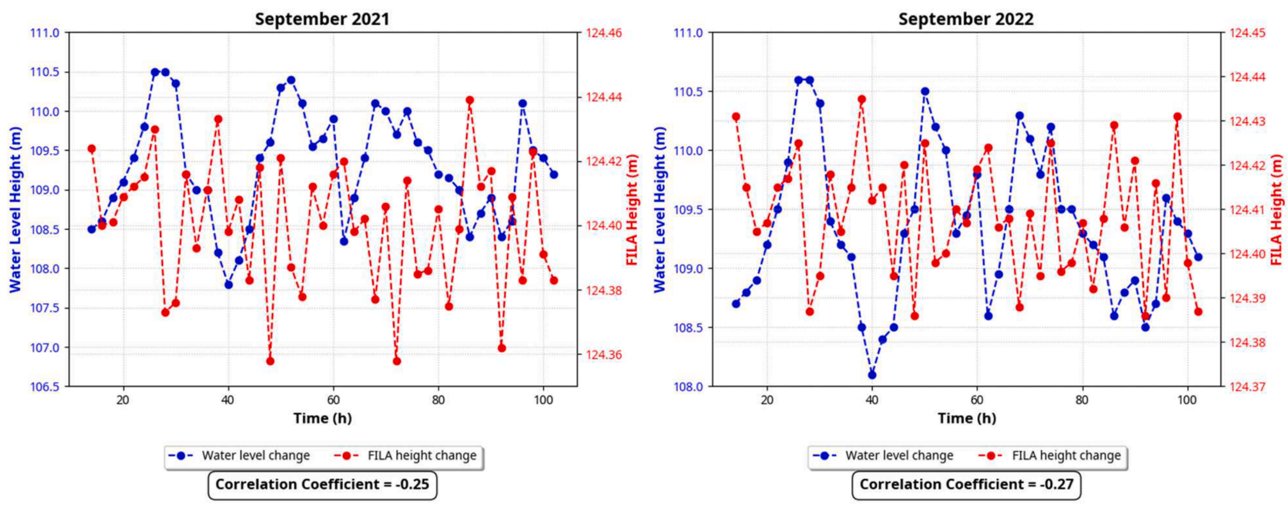

Fig. 7. shows the inverse relationship between water level fluctuations and FILA station elevation during the September 2021 and September 2022 (flood season) campaigns. Rapid water level changes from dam operations are correlated with short-term elevation decreases, indicating the island's immediate sensitivity to sudden water discharge events during the flood season.

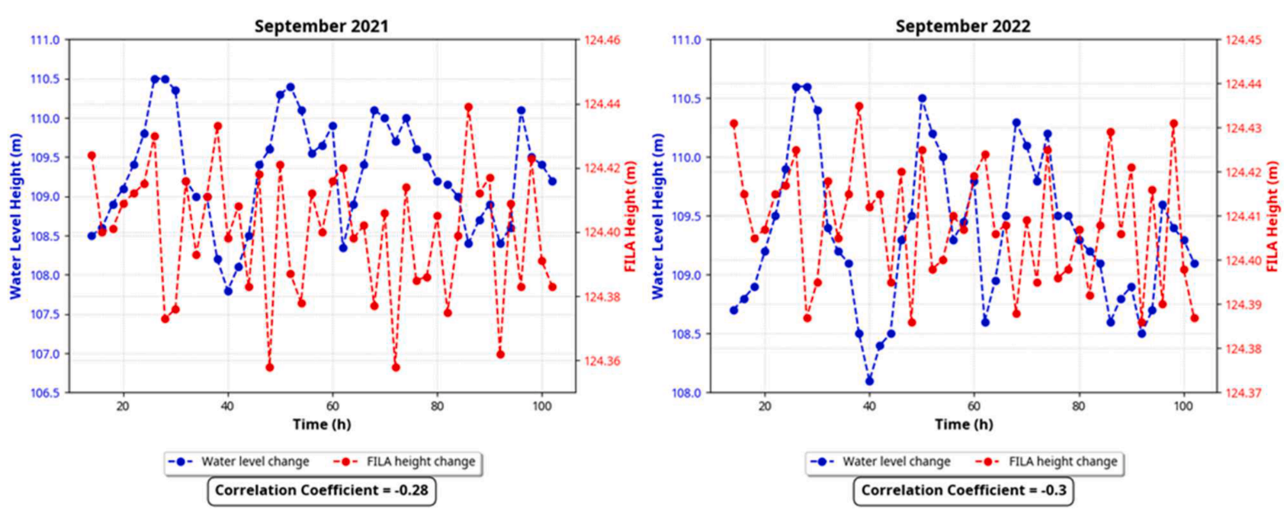

Fig. 8. shows the enhanced inverse relationship between FILA station elevation and water level with a 4-hour delay in the September 2021 and 2022 campaigns. The findings highlight a quicker hydro-mechanical response during flood season, underscoring the impact of rapid dam-controlled water level fluctuations on short-term ground deformation.

Table 3
Summary of elevation changes, water level (WL) fluctuations, and correlation results from GPS campaigns at Philae Island. The table compares dry and flood seasons, showing initial and lag-adjusted Pearson correlations and corresponding time delays.

Campaign Date	Season	Max Elevation (m)	Min Elevation (m)	Max WL (m)	Min WL (m)	Initial Corr.	Corr. with Lag	Lag Duration (h)
Mar. 2021	Dry	124.418	124.369	110.4	107.0	−0.105	−0.61	8
Sep. 2021	Flood	124.43	124.398	110.6	107.9	−0.25	−0.28	4
Feb. 2022	Dry	124.422	124.386	109.3	107.1	−0.234	−0.59	8
Sep. 2022	Flood	124.439	124.384	110.7	108.1	−0.27	−0.30	4
Mar. 2023	Dry	124.419	124.374	110.2	107.9	−0.264	−0.73	8

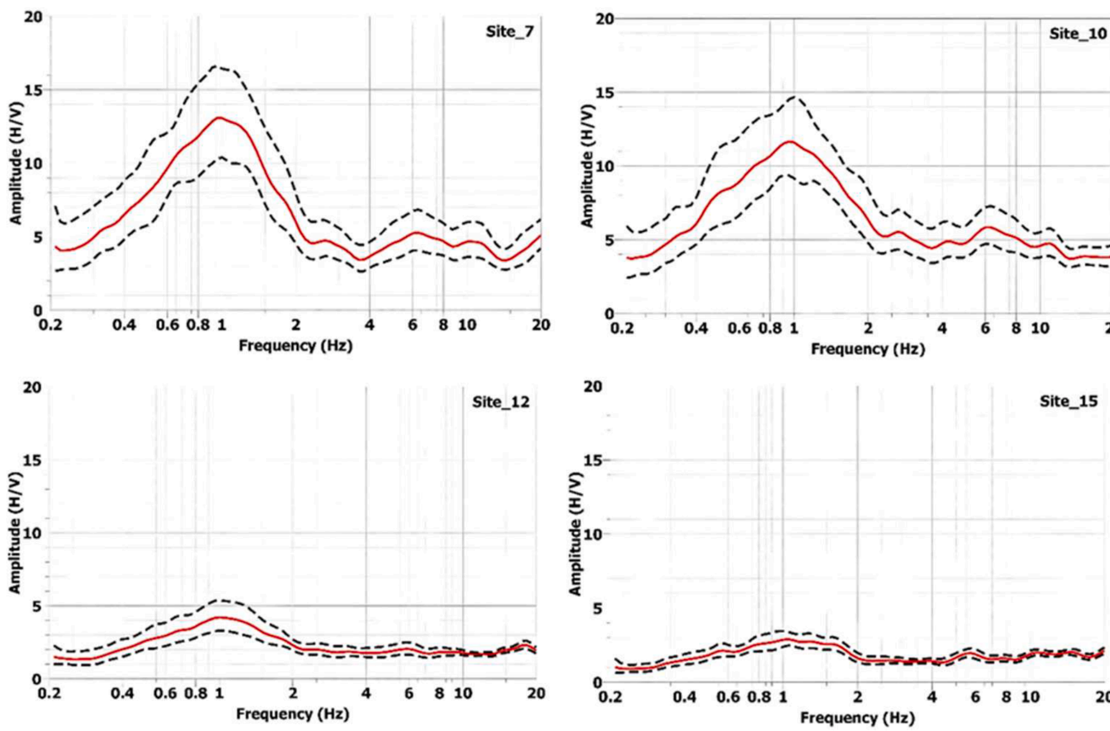

Fig. 9. displays H/V spectral curves from different sites on Philae Island, showing distinct single peaks at different frequencies. These peaks indicate the fundamental resonance frequencies of the local subsurface. The red lines indicate the average H/V response, aiding in identifying areas with potential seismic amplification risk.

temple shows high amplitude values ranging from 12 to 13.5 at points 5, 8, and 9. These high amplitude values are related to the usage of a large amount of granitic rocks combined with some silt sediment in the settling of the island's surface. The impedance contrast between the overlying cover and the bedrock controls the site amplification level, with areas having higher amplification values exhibiting higher impedance contrast values.

The seismic vulnerability index (Kg) on the island varies from 4 to 193, as depicted in (Fig. 12). This index is based on the interpretations of A_0 and F_0. The distribution of the seismic vulnerability index (Kg) aligns with the general trend of the amplification factor (A_0) distribution shown in (Fig. 11b). This indicates that locations with significant amplification factors tend to have higher seismic vulnerability. However, the distribution of the predominant frequency (F_0), as illustrated in (Fig. 11a), follows an opposite pattern.

6. Discussion

This study successfully integrated GPS and microtremor measurements to assess the impact of water level changes and evaluate the seismic vulnerability of Philae Is-land. The GPS analysis revealed a significant inverse correlation between water level variations and elevation changes at the FILA station, situated on the island itself. Specifically, during dry seasons (March 2021, February 2022, and March 2023), correlation coefficients between water level and elevation changes were −0.105, −0.234, and −0.264, respectively. These values demonstrate a clear trend: as water levels rise, the island experiences subsidence, and conversely, as water levels decrease, the island undergoes uplift.

A crucial finding was the temporal delay in the island's elevation response to water level fluctuations. When accounting for an 8-hour delay, the inverse correlation coefficients significantly increased to −0.61, −0.59, and −0.73 for the same dry season campaigns. This suggests that the island's response is not instantaneous but rather a gradual adaptation to the changing water loads. This delayed reaction underscores the complex hydro mechanical interactions between the fluctuating water levels and the island's geological substrate.

During the Nile flood season (September 2021 and September 2022), the correlation coefficients were −0.25 and −0.27, respectively. The rapid water level changes during this period, due to dam gate operations, resulted in a more immediate impact on the island's elevation. A 4-hour delay in water level changes yielded correlation coefficients of −0.28 and −0.3, indicating that the island's response is more rapid during periods of rapid water level fluctuation. This highlights the dynamic influence of water management practices on the island's stability.

To clarify the key differences between monitoring scales, Table 4 summarizes the key findings from the short-term (sub-daily) and seasonal-scale GPS campaigns. It illustrates how the temporal resolution of measurements influences the observed deformation patterns and correlation behavior at Philae Island [64].

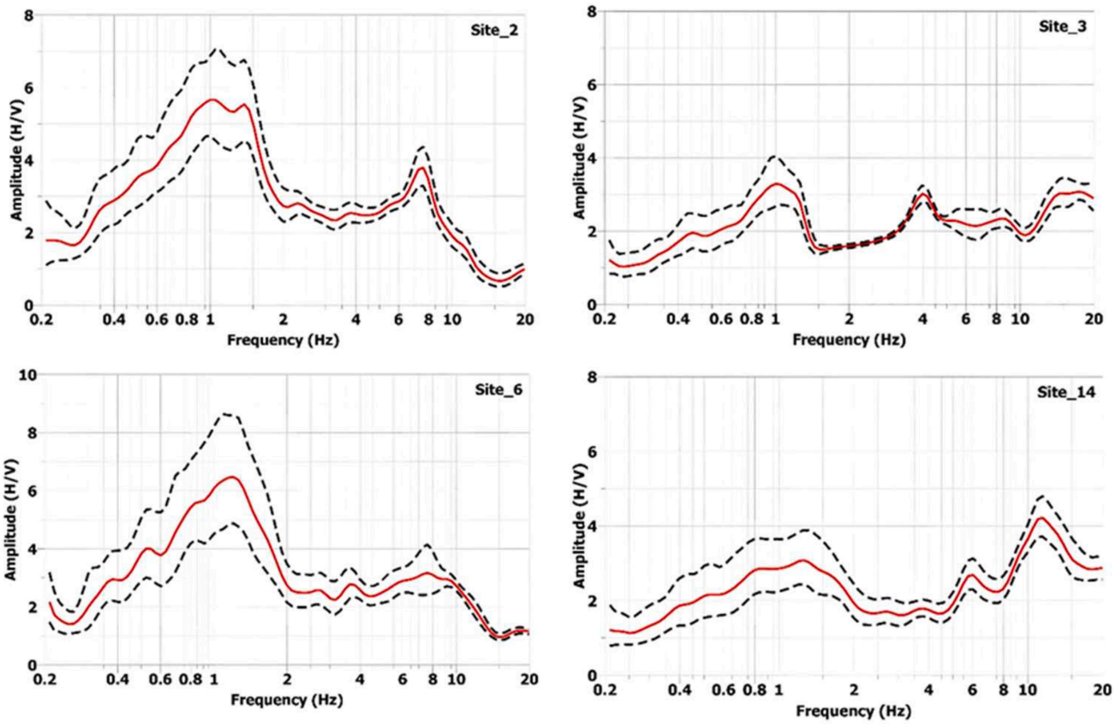

Fig. 10. shows multiple peaks in H/V spectral ratio curves from different sites on Philae Island, indicating complex subsurface layering and impedance contrasts likely due to the reshaping of Agilkia Island with granitic blocks and silt. The red lines show average H/V values.

The microtremor measurements, analyzed using the HVSR technique, provided valuable insights into the seismic vulnerability of the Philae Temple structures. The fundamental frequency (F_0) values ranged from 0.92 to 1.22 Hz across the 16 measurement sites. The east-central sections of the island exhibited lower F_0 values (<1 Hz), indicating softer soil deposits and fractured granite, which are more susceptible to ground motion amplification. Conversely, the northern and southern parts of the island showed higher F_0 values (1.1 to 1.22 Hz), suggesting more stable ground conditions.

The peak amplitude (A_0) of the H/V ratio varied significantly, ranging from 2 to 13.5. The middle and northwestern parts of the island displayed the highest A0 values, indicating significant impedance contrasts and, consequently, higher ground motion amplification. Specifically, points 5, 8, and 9 exhibited A_0 values ranging from 12 to 13.5, likely due to the use of granitic rocks and silt in reshaping the island.

The seismic vulnerability index (Kg), calculated from F_0 and A_0, ranged from 4 to 193. This index highlights areas with higher amplification factors, which generally exhibit higher seismic vulnerability. The distribution of Kg closely followed the trend of A_0, reinforcing the importance of understanding local ground conditions for assessing structural risks. Our Kg values are consistent with those observed at other reshaped or sediment-amplified archaeological sites, such as Pompeii and Machu Picchu. These sites exhibit complex subsurface conditions and anthropogenic fill materials, which enhance ground motion and increase seismic vulnerability. In the case of Agilkia Island, the reconstruction involved both granite blocks and silt infill, creating notable contrasts in material density that are likely more pronounced than in natural fluvial settings. Such heterogeneity may intensify local site effects. The Kg seismic vulnerability index used in this study is a widely recognized, dimensionless parameter for assessing the potential for seismic amplification at specific locations. Our findings suggest that certain reconstructed zones may be subject to elevated ground motion during seismic events, underscoring the importance of focused conservation strategies in those areas.

Agilkia Island's anthropogenic composition, comprising relocated granite blocks interlaid with soft silt fill, differs markedly from naturally stratified geological settings. The resulting sharp impedance contrasts can lead to stronger ground shaking compared to natural soils, where sediment transitions are typically more gradual. These reconstructed layers create localized amplification zones, particularly in areas where shallow, low-velocity materials are interspersed with denser granite. This effect is evident in the elevated Kg values and pronounced HVSR peak amplitudes observed in the central and northwestern sectors of the island. Such engineered configurations exacerbate site-specific seismic responses and must be carefully accounted for in future risk mitigation strategies and restoration planning.

Previous studies on heritage sites have mainly focused on either hydrological or seismic risks, but few have examined short-term time-delayed responses to water loading with the level of detail shown in this study. For example, research at Angkor Wat in Cambodia and Machu Picchu in Peru concentrated on long-term slope stability or resonance mapping without identifying any delayed correlation between water fluctuations and vertical displacement [65,66]. Similarly, studies in dam-affected archaeological areas in Italy and the Eastern Mediterranean highlighted the impact of fluctuating water tables but lacked high frequency GPS data to quantify these effects over hourly timescales. In contrast, our study reveals an 8-hour delay in elevation response during dry seasons and a 4-hour delay during flood conditions, providing new evidence of gradual hydro-mechanical adjustment at heritage sites with engineered water systems. This temporal sensitivity enhances our understanding of site-specific deformation dynamics in response to external water loads.

Comparing our approach with similar studies highlights the effectiveness of the integrated GPS and microtremor method used on Philae Island. For instance, Maeda et al. conducted a microtremor analysis at Angkor Wat to assess seismic risk but lacked continuous GPS monitoring for temporal analysis [65]. Similarly, Galassi et al. assessed seismic risk at Cumae in Italy using HVSR and vulnerability indexing but did not con-sider hydrological influences or time-dependent deformation [66]. In contrast, our study combines HVSR-derived parameters with GPS analysis to evaluate the island's response to water level fluctuations, offering a more comprehensive risk assessment model for heritage sites

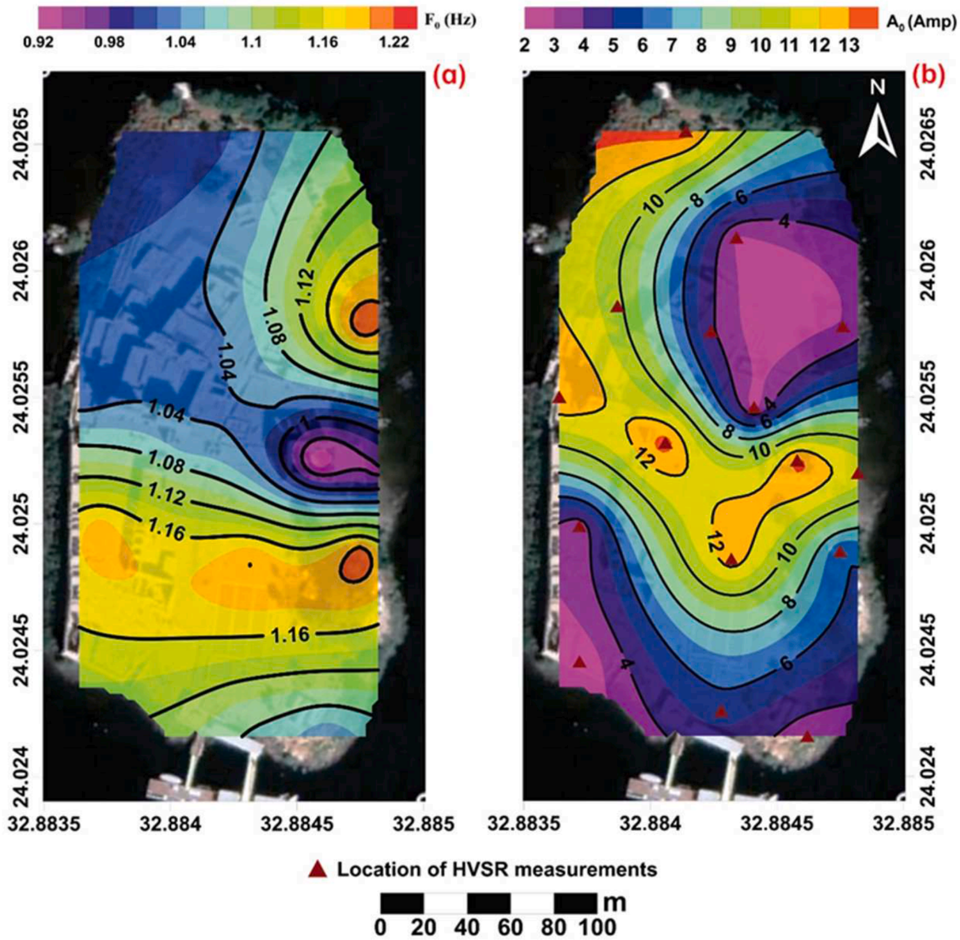

Fig. 11. (a) Zonation map illustrating the spatial distribution of fundamental frequency (*F₀*) values obtained from HVSR analysis. The presence of lower frequencies (<1 Hz) in the east and central zone indicates the presence of softer sediment layers and fractured granite, suggesting a higher vulnerability to seismic amplification. (b) Zonation map displaying H/V amplitude (A_o) values associated with F₀, pinpointing regions with elevated ground motion amplification, particularly in the middle and northwestern parts of the island, attributed to substantial impedance variations in subsurface materials.

affected by seismic and hydrological factors. In addition to our focus on surface water changes, we recognize that groundwater movement through basement rock fractures may also influence the observed deformation. The site's lithology suggests that groundwater likely flows along confined local paths controlled by fracture arrangement and connectivity. To better isolate the effects of subsurface water in future studies, we recommend incorporating piezometric logging, groundwater level monitoring, and the development of detailed fracture-based flow models. Although groundwater data were not available in the current study, such measurements would be essential for a more comprehensive hydro-mechanical interpretation [67]. Additionally, employing terrestrial laser scanning [68] to create a high-resolution 3D model of the temple would enhance archival recording, structural integrity assessment, and preservation planning.

Finally, considering the increasing frequency of extreme hydrological events driven by climate change, long-term monitoring strategies should incorporate future flood risk projections. Employing scenario models based on Coupled Model Intercomparison Project Phase 6 (CMIP6) climate pathways can support forecasting of stress exposure and enhance resilience planning for Philae Island. Integrating such climate-informed projections aligns with recent international recommendations to safeguard cultural heritage sites through proactive, risk-based adaptation strategies [69].

7. Conclusions

This study examined the impact of water level fluctuations on Philae Island stability and assessed the seismic vulnerability of its structures using GPS monitoring and microtremor measurements. The results revealed a clear inverse correlation between water level changes and elevation variations at the FILA station on Philae Island. As water levels increased, gradual subsidence was observed, whereas decreasing water levels led to uplift, with a time-lagged response, indicating that the island's elevation responds gradually to changes in water load.

Additionally, seasonal variations and rapid water level changes caused by dam operations were found to significantly affect the island's elevation. Microtremor measurements identified zones of potential seismic vulnerability, where impedance contrast between surface materials and bedrock resulted in lower fundamental frequencies and higher ground motion amplification, posing potential risks to the temple structures.

While our primary investigation focused on the direct and evident relationship with surface water level changes, it is important to acknowledge the potential for mi-nor groundwater influence. Given the island's predominant basement rock composition, groundwater is typically confined to fracture systems. Quantifying its precise contribution to observed elevation changes would necessitate detailed, site-specific hydrogeological investigations, including piezometric monitoring within the island's fracture network, which could be an avenue for future dedicated studies.

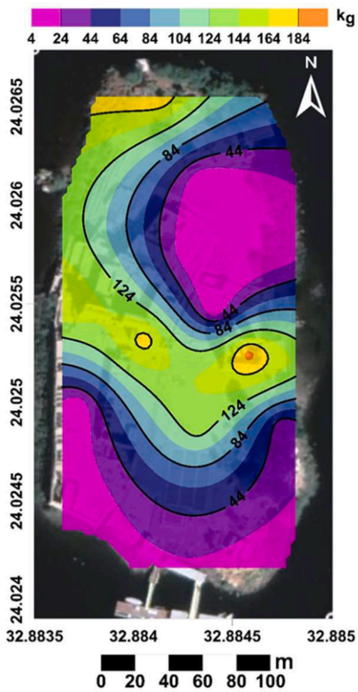

Fig. 12. shows the seismic vulnerability index (Kg) distribution on Philae Island, highlighting areas with different levels of susceptibility to seismic amplification. Higher Kg values in the central and northwestern regions indicate higher ground motion amplification and structural vulnerability.

Table 4
Comparative summary of insights from short-term (sub-daily) and seasonal-scale GPS monitoring at Philae Island, emphasizing differences in measurement time frames, correlation patterns, and implications for geophysical interpretation.

Insight Type	Monitoring Scale	Key Observation	Correlation Behavior	Interpretation
Short term	Sub-daily (2 h.)	Delayed elevation drops following water rise	Stronger inverse correlation with 4–8 h. lag	Indicates time-dependent elastic or pyroclastic response to water load
Seasonal scale	Monthly/ seasonal	Gradual deformation linked to long-term water trends	Weak to moderate inverse correlation (no lag)	Suggests broader hydraulic loading effect with seasonal impact

To enhance the preservation and monitoring of Philae Island, this study recommends a multifaceted approach. Integrating GPS data with precise leveling and satellite imagery would significantly improve long-term deformation assessments. For increased positional accuracy, GPS data were processed using reference data from IGS stations. To expand spatial coverage beyond the current GPS network, future work will incorporate Sentinel-1 InSAR time-series data. This will enable the mapping of continuous deformation patterns across the island and validation of GPS derived trends using complementary geodetic techniques. Furthermore, establishing permanent GPS station on Philae Island is planned to support high-resolution, long-term monitoring. The integration of both satellite-based and ground-based observations will be essential for comprehensive risk assessments and informed heritage conservation planning. A multidisciplinary collaboration involving geotechnical and civil engineers is crucial for evaluating soil characteristics and mitigating potential risks to the temple structures. Finally, to enable real-time monitoring and support proactive heritage conservation, a digital replica of the Philae Temple could be developed in future efforts. This digital twin would integrate high-resolution 3D laser scanning, IoT-enabled deformation sensors, and predictive modeling tools. Such a system would simulate the temple's structural behavior, continuously monitor environmental and mechanical stressors, and provide early warnings when conservation interventions are required.

Abbreviations

A_0	Peak Amplitude (Horizontal to Vertical Ratio)
CMIP6	Coupled Model Intercomparison Project Phase 6
F_0	Fundamental Frequency
GPS	Global Positioning System
HVSR	Horizontal to Vertical Spectral Ratio
IGS	International GNSS Service
Kg	Vulnerability Index
SD	Standard Deviation

Funding

This research did not receive any specific grant from funding agencies in the public, commercial, or not-for-profit sectors.

CRediT authorship contribution statement

Abdelhamid Elbshbeshi: Writing – original draft, Visualization, Software, Resources, Methodology, Investigation, Funding acquisition, Formal analysis, Data curation, Conceptualization. **Ismael M. Ibraheem:** Writing – review & editing, Visualization, Validation, Resources, Project administration, Funding acquisition. **Ahmed Gomaa:** Writing – original draft, Validation, Methodology, Investigation, Formal analysis, Data curation, Conceptualization. **Abdelmonem Mohamed:** Writing – review & editing, Supervision, Methodology, Investigation, Formal analysis, Conceptualization. **Amal Othman:** Writing – review & editing, Supervision, Resources, Formal analysis, Data curation. **Hosni Ghazala:** Writing – review & editing, Validation, Supervision, Project administration, Investigation, Conceptualization.

Declaration of competing interest

The authors declare no conflicts of interest.

Acknowledgments

The authors would also like to express their sincere gratitude to the Egyptian Ministry of Tourism and Antiquities for granting the necessary permissions to access and carry out measurements at the Philae temples. Their cooperation was essential to the successful completion of this study.

Data availability

The original contributions presented in this study are included in the article. Further inquiries can be directed to the first author.

References

[1] A.R. Mamo, I.M. Ibraheem, A. Al Kassem, A. Al-Khalil, K. Hopper, The impact of the Syrian conflict on archaeological sites in Al-Hasakah Province, J. Archaeol. Sci. Rep. 43 (2022) 103486, https://doi.org/10.1016/j.jasrep.2022.103486.
[2] A. Elbshbeshi, A. Gomaa, A. Mohamed, A. Othman, H. Ghazala, Seismic hazard evaluation by employing microtremor measurements for Abu Simbel area, Aswan, Egypt, J. Afr. Earth Sci. 196 (2022) 104734, https://doi.org/10.1016/j.jafrearsci.2022.104734.
[3] A. Al Kassem, K. Hopper, I.M. Ibraheem, H.el Hajj, A. Maier, A.A. Ali, J. Richter, Assessment of the impact of the Syrian conflict on archaeological sites in the Daraa region, Levant. 56 (3) (2024) 425–446, https://doi.org/10.1080/00758914.2024.2420409.
[4] C. Polykretis, D.D. Alexakis, M.G. Grillakis, A. Agapiou, B. Cuca, N. Papadopoulos, A. Sarris, Assessment of water-induced soil erosion as a threat to cultural heritage

sites: the case of Chania prefecture, Crete Island, Greece, Big. Earth. Data 6 (4) (2021) 561–579, https://doi.org/10.1080/20964471.2021.1923231.

[5] I. Schmidt, B. Boemke, H. Herzog, C. Koppmann, H. Witte, F. Sauer, E. Claßen, F. Lehmkuhl, Assessing the impact of the 2021 flood event on the archaeological heritage of the Rhineland (Germany), Environ. Sci. Eur. 36 (1) (2024) 164, https://doi.org/10.1186/s12302-024-00991-w.

[6] A. Giammarusti, The two islands of Philae: a memory of the temples relocation, Remembering the "Nubia Campaign": Recollect. Evaluat. Int. Campa. Save Monume. Nubia After Fifty Years (2024) 141. –118.

[7] H. Kockelmann, Jenseitsgericht Und Priesterweihe: Ein singuläres Zeugnis für die Tür als Ort der Rechtfertigung und Initiation aus Der Tempelanlage von Philae, Bulletin de l'Institut français d'archéologie orientale (BIFAO), 2025, pp. 249–277, https://doi.org/10.4000/148rr.

[8] K.R. Olson, G.K. Kome, Review and analysis of Africa's lifelines: the Nile River and the Aswan High Dam, Open J. Soil Sci. 14 (12) (2024) 741–764, https://doi.org/10.4236/ojss.2024.1412036.

[9] N. Sushma, H.N. Suresh, L.J. Mohana, K.S. Kumar, Experimental investigation on wireless integrated smart system for energy and water resource management in Indian smart cities, Results. Eng. 23 (2024) 102687, https://doi.org/10.1016/j.rineng.2024.102687.

[10] X. Fan, Earthquake-induced chains of geologic hazards, in: AGU Fall Meeting Abstracts 2019, 2019. EP53B–02.

[11] S.S. Lin, S.L. Shen, A. Zhou, Y.S. Xu, Risk assessment and management of excavation system based on fuzzy set theory and machine learning methods, Autom. Constr. 122 (2021) 103490, https://doi.org/10.1016/j.autcon.2020.103490.

[12] G. Gurbuz, B. Aktug, S. Jin, S.H. Kutoglu, A GNSS-based near real time automatic Earth crust and atmosphere monitoring service for Turkey, Adv. Space Res. 66 (12) (2020) 2854–2864, https://doi.org/10.1016/j.asr.2020.07.026.

[13] A. Ramya, R. Poornima, G. Karthikeyan, S. Priyatharshini, K.G. Thanuja, P. Dhevagi, Climate-induced and geophysical disasters and risk reduction management in mountains regions. Climate Change Adaptation, Risk Management and Sustainable Practices in the Himalaya, Springer International Publishing, Cham, 2023, pp. 361–405, https://doi.org/10.1007/978-3-031-24659-3_16.

[14] V. Sakkas, Ground deformation modelling of the 2020 Mw6. 9 Samos earthquake (Greece) based on InSAR and GNSS data, Remote Sens. (Basel) 13 (9) (2021) 1665, https://doi.org/10.3390/rs13091665.

[15] G. Wang, The 95% confidence interval for GNSS-derived site velocities, J. Survey. Eng. 148 (1) (2022) 04021030. https://orcid.org/0000-0003-3731-3839.

[16] M. Alvioli, G. Falcone, A. Mendicelli, F. Mori, F. Fiorucci, F. Ardizzone, M. Moscatelli, Seismically induced rockfall hazard from a physically based model and ground motion scenarios in Italy, Geomorphology 429 (2023) 108652, https://doi.org/10.1016/j.geomorph.2023.108652.

[17] J. Van Ginkel, E. Ruigrok, R. Wentinck, R. Herber, Amplification behaviour of compressional waves in unconsolidated sediments, Front. Earth. Sci. (Lausanne) 10 (2022) 812658, https://doi.org/10.3389/feart.2022.812658.

[18] Y. Nakamura, A method for dynamic characteristics estimation of subsurface using microtremor on the ground surface, Railway Tech. Res. Inst. Quarterly Rep. 30 (1) (1989). http://worldcat.org/oclc/3127232.

[19] Ş.Ç. Tuna, Probabilistic assessment of soil liquefaction-induced failures during the 2023 Kahramanmaraş earthquakes in Türkiye: a case study from Iskenderun city, Soil Dyn. Earthquake Eng. 199 (2025) 109661, https://doi.org/10.1016/j.soildyn.2025.109661.

[20] Z. Al-Ibraheemi, S. Al-Janabi, Sustainable energy: advancing wind power forecasting with grey wolf optimization and GRU models, Results. Eng. 24 (2024) 102930, https://doi.org/10.1016/j.rineng.2024.102930.

[21] L. Nardone, M. Vassallo, G. Cultrera, V. Sapia, S. Petrosino, M. Pischiutta, A. Tramelli, A geophysical multidisciplinary approach to investigate the shallow subsoil structures in volcanic environment: the case of Ischia Island, J. Volcanol. Geothermal Res. 438 (2023) 107820, https://doi.org/10.1016/j.jvolgeores.2023.107820.

[22] L. La Mendola, M. Accardi, F. Agnello, A. Monaco, Path of knowledge for the assessment of structural safety of the Pisan Tower of the royal palace of Palermo in Italy, Heritage 6 (8) (2023) 5818–5847, https://doi.org/10.3390/heritage6080306.

[23] V. Amato, M. Covolan, H. Dessales, A. Santoriello, Seismic microzonation of the Pompeii archaeological Park (southern Italy): local seismic amplification factors, Geosciences. (Basel) 12 (7) (2022) 275, https://doi.org/10.3390/geosciences12070275.

[24] F. Zaina, D. Tapete, Satellite-based methodology for purposes of rescue archaeology of cultural heritage threatened by dam construction, Remote Sens. (Basel) 14 (4) (2022) 1009, https://doi.org/10.3390/rs14041009.

[25] S.P. Putti, N. Satyam, Evaluation of site effects using HVSR microtremor measurements in Vishakhapatnam (India), Earth. Syst. Environ. 4 (2020) 439–454, https://doi.org/10.1007/s41748-020-00158-6.

[26] Canuti, P.; Margottini, C.; Mucho, R.; Casagli, N.; Delmonaco, G.; Ferretti, A.; Tarchi, D. Preliminary remarks on monitoring, geomorphological evolution and slope stability of Inca Citadel of Machu Picchu (C101-1), Landslides: risk analysis and sustainable disaster management. 2005, 39–47. https://doi.org/10.1007/3-540-28680-2_3.

[27] I. Khadrouf, O. El Hammoumi, N. El Goumi, M. Oukassou, Contribution of HVSR, MASW, and geotechnical investigations in seismic microzonation for safe urban extension: a case study in Ghabt Admin (Agadir), western Morocco, J. African Earth Sci. 210 (2024) 105138, https://doi.org/10.1016/j.jafrearsci.2023.105138.

[28] M. Katsianis, E. Gkadolou, linking the Greek experience with wider research considerations, 9 archaeological and cultural heritage web mapping resources, Archaeol. Rep. 70 (2024) 213–238, https://doi.org/10.1017/S0570608424000036.

[29] S. Ge, M.O. Saar, Induced seismicity during geo energy development A hydromechanical perspective, J. Geophys. Res. Solid Earth 127 (3) (2022), https://doi.org/10.1029/2021JB023141 e2021JB023141.

[30] S.R. Vadyala, S.N. Betgeri, J.C. Matthews, E. Matthews, A review of physics-based machine learning in civil engineering, Results. Eng. 13 (2022) 100316, https://doi.org/10.1016/j.rineng.2021.100316.

[31] N. Adamo, N. Al-Ansari, V. Sissakian, J. Laue, S. Knutsson, Geophysical methods and their applications in dam safety monitoring, J. Earth Sci. Geotech. Eng. 11 (1) (2021) 291–345, https://doi.org/10.47260/jesge/1118.

[32] S. Nicolini, Reconstructing the archaeological landscape of Shellal in the region of the first Nile cataract, East West 4 (1) (2023) 65–84. https://www.jstor.org/stable/48774246.

[33] A. Alhowaily, Revitalizing urban governance: integrating smart growth and decolonial perspectives for municipal empowerment in shaping growth across Egyptian desert landscapes, J. Contemporary Urban Affairs 7 (2) (2023) 244–261, https://doi.org/10.25034/ijcua.2023.v7n2-15.

[34] M.A. Azeem, M. Mekkawi, M. Gobashy, Subsurface structures using a new integrated geophysical analysis, South Aswan, Egypt, Arabian J. Geosci. 7 (2014) 5141–5157, https://doi.org/10.1007/s12517-013-1140-x.

[35] G.R. Foulger, M.P. Wilson, J.G. Gluyas, B.R. Julian, R.J. Davies, Global review of human-induced earthquakes, Earth. Sci. Rev. 178 (2018) 438–514, https://doi.org/10.1016/j.earscirev.2017.07.008.

[36] B. Issawi, An introduction to the physiography of the Nile Valley. Prehistory of the Nile Valley, Academic Press, 1976, pp. 3–22, https://doi.org/10.1016/B978-0-12-743950-1.50009-X.

[37] S. Kele, E.S. Sallam, E. Capezzuoli, M. Rogerson, H. Wanas, C.C. Shen, K. W. Huntington, Were springline carbonates in the Kurkur–Dungul area (southern Egypt) deposited during glacial periods? J. Geol. Soc. London. 178 (3) (2021) https://doi.org/10.1144/jgs2020-147 jgs2020–147.

[38] A.S. Mohamed, G.H. Hassib, N. AbouAly, A. El-Kutb, Evaluation of recent crustal deformation and seismicity in spillway fault area, Aswan, Egypt, NRIAG Journal of Astron. Geophys. 11 (1) (2022) 325–336, https://doi.org/10.1080/20909977.2022.2106667.

[39] M.A. Hamdan, F.A. Hassan, Quaternary of Egypt, in: Z. Hamimi, A. El-Barkooky, J. Martínez Frías, H. Fritz, Y. Abd El-Rahman (Eds.), The Geology of Egypt. Regional Geology Reviews, Springer, Cham, 2020, pp. 445–493, https://doi.org/10.1007/978-3-030-15265-9_12.

[40] T. Tha, T. Piman, D. Bhatpuria, P. Ruangrassamee, Assessment of riverbank erosion hotspots along the mekong river in cambodia using remote sensing and hazard exposure mapping, Water. (Basel) 14 (13) (2022) 1981, https://doi.org/10.3390/w14131981.

[41] M.G. Wolman, C. Le Meur, R.F. Giegengack, The Nile River: geology, hydrology, Hydraulic Society, 2nd Edition, Geomorphology and Management, Large Rivers, 2022, pp. 704–736, https://doi.org/10.1002/9781119412632.ch24.

[42] M. El Bohoty, E. Ghamry, A. Hamed, M. Khalifa, A. Taha, A. Meneisy, Surface and subsurface structural mapping for delineating the active emergency spillway fault, Aswan, Egypt, using integrated geophysical data, Acta Geophys. 72 (2) (2024) 807–827, https://doi.org/10.1007/s11600-023-01133-1.

[43] P.A. Rosen, S. Hensley, I.R. Joughin, F.K. Li, S.N. Madsen, E. Rodriguez, R. M. Goldstein, Synthetic aperture radar interferometry, Proc. IEEE 88 (3) (2000) 333–382, https://doi.org/10.1109/5.838084.

[44] Y. Hussain, R. Schlögel, A. Innocenti, O. Hamza, R. Iannucci, S. Martino, H. B. Havenith, Review on the geophysical and UAV-based methods applied to landslides, Remote Sens. 14 (18) (2022) 4564, https://doi.org/10.3390/rs14184564.

[45] R. Sawires, J.A. Peláez, F. Sparacino, A.M. Radwan, M. Rashwan, M. Palano, Seismic and geodetic crustal moment-rates comparison: new insights on the seismic hazard of Egypt, Appl. Sci. 11 (17) (2021) 7836, https://doi.org/10.3390/app11177836.

[46] R.M. Kebeasy, A.A. Gharib, Active fault and water loading are important factors in triggering earthquake activity around Aswan Lake, J. Geodyn. 14 (1–4) (1991) 73–85, https://doi.org/10.1016/0264-3707(91)90010-C.

[47] D. Kuang, S.D. Desai, B.J. Haines, X. Wu, Point positioning the geocenter through LEO GPS tracking and its application in geophysics, GPS. Solut. 28 (3) (2024) 137, https://doi.org/10.1007/s10291-024-01680-0.

[48] L. Bastos, M. Bos, R.M. Fernandes, Deformation and tectonics: contribution of GPS measurements to plate tectonics–overview and recent developments, Sci. Geodesy-I: Adv. Future Direct. (2010) 155–184, https://doi.org/10.1007/978-3-642-11741-1_5.

[49] A. Rashidi, R. Derakhshani, Strain and moment rates from GPS and seismological data in northern Iran: implications for an evaluation of stress trajectories and probabilistic fault rupture hazard, Remote Sens. (Basel) 14 (9) (2022) 2219, https://doi.org/10.3390/rs14092219.

[50] A. Pirsiavash, A. Broumandan, G. Lachapelle, K. O'keefe, GNSS code multipath mitigation by cascading measurement monitoring techniques, Sensors 18 (6) (2018) 1967, https://doi.org/10.3390/s18061967.

[51] M. Nogoshi, T. Igarashi, On the amplitude characteristics of microtremor (part 2), J. Seism. Soc. Japan 24 (1971) 26–40.

[52] Y. Nakamura, A method for dynamic characteristics estimation of subsurface using microtremor on the ground surface, Railway Technical Research Institute, Quarterly Reports 30 (1) (1989) 25–33.

[53] M. Ibs-von Seht, J. Wohlenberg, Microtremor measurements used to map thickness of soft sediments, Bull. Seismol. Soc. Am. 89 (1) (1999) 250–259, https://doi.org/10.1785/BSSA0890010250.

[54] K. Atakan, The need for standardized approach for estimating the local site effects based on ambient noise recordings. Increasing Seismic Safety By Combining Engineering Technologies and Seismological Data, Springer Netherlands, Dordrecht, 2009, pp. 3–15, https://doi.org/10.1007/978-1-4020-9196-4_2.
[55] Y. Nakamura, Clear identification of fundamental idea of Nakamura's technique and its applications, in: Proceedings of the 12th world conference on earthquake engineering. 2656, 2000, pp. 1–8.
[56] C. Acerra, G. Aguacil, A. Anastasiadis, K. Atakan, R. Azzara, P.Y. Bard, S. Bonnefoy-Claudet, Guidelines for the implementation of the H/V spectral ratio technique on ambient vibrations measurements, processing and interpretation, European Commission EVG1-CT- 2000-00026 SESAME. https://orbi.uliege.be/bitstream/2268/250698/1/HV_User_Guidelines.pdf, 2004.
[57] A. Elbshbeshi, M.*Sc*. Thesis, Geology Department, Faculty of Science, Mansoura university, 2018.
[58] Y. Nakamura, Seismic vulnerability indices for ground and structures using microtremor, in: World congress on railway research in Florence, Italy, 1997, pp. 1–7.
[59] R. Dach, Bernese GNSS Software Version 5.2, User manual/Publikation Digital AG, 2015, https://doi.org/10.7892/boris.72297.
[60] M. Soliman, D. Ali, A. Elbshbeshi, M.G. Ibrahim, Digitization of Qaitbay Fort in Alexandria (884AH/1479 CE) -simplification of modelling techniques to safeguard vulnerable cultural heritage, Art Res. J. 25 (3) (2025) 109–121.
[61] K. Konno, T. Ohmachi, Ground-motion characteristics estimated from spectral ratio between horizontal and vertical components of microtremor, Bull. Seismol. Soc. Am. 88 (1) (1998) 228–241, https://doi.org/10.1785/BSSA0880010228.
[62] S.S. Moustafa, M.S. Abdalzaher, F. Khan, M. Metwaly, E.A. Elawadi, N.S. Al-Arifi, A quantitative site-specific classification approach based on affinity propagation clustering, IEEE Access. 9 (2021) 155297–155313, https://doi.org/10.1109/ACCESS.2021.3128284.
[63] S.Y. Kang, K.H. Kim, B. Kim, Assessment of seismic vulnerability using the horizontal-to-vertical spectral ratio (HVSR) method in Haenam, Korea, Geosci. J. 25 (2021) 71–81, https://doi.org/10.1007/s12303-020-0040-9.
[64] M.A. Sutton, Digital image correlation for shape and deformation measurements. Springer Handbook of Experimental Solid Mechanics, Springer, Boston, MA, 2008, pp. 565–600, https://doi.org/10.1007/978-0-387-30877-7_20.
[65] T. Maeda, Y. Sugiura, T. Hirai, FEM modeling of the towers in Bayon temple in Cambodia based on micro-tremor measurements, Adv. Eng. Softw. 39 (4) (2008) 346–355, https://doi.org/10.1016/j.advengsoft.2007.01.007.
[66] S. Galassi, N. Ruggieri, G. Tempesta, A novel numerical tool for seismic vulnerability analysis of ruins in archaeological sites, Int. J. Arch. Heritage 14 (1) (2020) 1–22, https://doi.org/10.1080/15583058.2018.1492647.
[67] R. Syah, J.W.G. Guerrero, A.L. Poltarykhin, W. Suksatan, S. Aravindhan, D. O. Bokov, W.K. Abdelbasset, S. Al-Janabi, A.F. Alkaim, D.Y. Tumanov, Developed teamwork optimizer for model parameter estimation of the proton exchange membrane fuel cell, Energy Rep. 8 (2022) 10776–10785, https://doi.org/10.1016/j.egyr.2022.08.177.
[68] A. Elbshbeshi, A. Gomaa, A. Mohamed, A. Othman, I.M. Ibraheem, H. Ghazala, Applying geomatics techniques for documenting heritage buildings in Aswan Region, Egypt: a case study of the temple of Abu Simbel, Heritage 6 (2023) 742–761, https://doi.org/10.3390/heritage6010040.
[69] H. Meresa, B. Tischbein, T. Mekonnen, Climate change impact on extreme precipitation and peak flood magnitude and frequency: observations from CMIP6 and hydrological models, Natural Hazards 111 (3) (2022) 2649–2679, https://doi.org/10.1007/s11069-021-05152-3.